Institute of Space and Aeronautical Science, University of Tokyo
Report No. 565, December 1978

Laminar Boundary Layer with Foreign Gas Injection on a Conical Body*

By

Kenichi MATSUNO** and Ryuma KAWAMURA

Abstract: The present paper deals with the theory of laminar boundary layer on a nonaxisymmetric conical body at supersonic flight with special reference to the effect of foreign gas injection (or "mas injection") on the body surface. The over-all flowfield over the conical body with nearly circular but otherwise arbitrary cross-section at small angles of attack is analytically solved using small perturbation method. The inviscid flow solution served as boundary layer edge conditions is obtained by an extension of the Stone's solution for a circular cone to the cases of nonaxisymmetric conical bodies. The similar boundary layer equations with a specific distribution of the mass injection rate inversely proportional to the square root of the meridional distance from the body apex are derived for the case of a binary mixture of nonreacting gases. An exact, first order perturbation solution not depending on flow parameters is presented, corresponding to the inviscid conical flow solution.

The effects of mass injection on three-dimensional boundary layer characteristics are discussed for the cases of several shapes of conical bodies. The analytical results demonstrate a significant effect of mass injection on the boundary layer flow, especially on the local heat transfer and skin friction.

NOMENCLATURE

c_i:	Mass fraction of injected gas
c_p:	Specific heat at constant pressure
D_{if}:	Binary diffusion coefficient
f_w:	Injection rate parameter
f, g:	Three-dimensional stream functions (see Eq. (2.17))
k:	Thermal conductivity
M_∞:	Freestream Mach Number
M_f^*:	Molecular weight of freestream gas, air
M_i^*:	Molecular weight of injected gas
N:	Chapman-Rubesin Number (see Eq. (2.17))
p:	Pressure
P_r:	Prandtl Number (see Eq. (2.7))

* This work was accomplished as the Doctorial thesis of K. Matsuno under the guidance of Prof. R. Kawamura at I.S.A.S. during the period from 1975 to 1977.

** National Aerospace Laboratory, 1880, Jindaiji, Chofu, Tokyo.

q: Local heat transfer
S_c: Schmidt Number (see Eq. (2.7))
t, T: Temperature
$T_{t\infty}$: Freestream reservoir temperature
x, y, s: Boundary layer coodinate system (see Fig. 1)
r, θ, φ: Spherical polar coodinate system (see Fig. 2)
u, v, w: Velocity components along x, y, s axes or r, θ, φ axes (see Figs. 1–2)
α: Angle of attack
β_1: $=c_{pi}-1$ (see Eq. (2.7))
β_2: $=M_f^*/M_i^*-1$ (see Eq. (2.8))
γ: Ratio of specific heats of freestream, air
ε_n, E_n: Fourie coefficients of the body (see Eq. (3.1))
ζ: $=s$ (see Eqs. (2.10)–(2.12))
$\bar{\theta}_b$: Semi-apex angle of the basic circular cone
$\bar{\theta}_s$: Semi-apex angle of the axisymmetric conical shock wave
θ_{sn}, Θ_{sn}: Fourie coefficients of the conical shock wave (see Eq. (3.23))
λ: Parabolic similarity variable
μ: Viscosity coefficient
ρ: Density
τ_x: Meridional skin friction
τ_φ: Circumferential skin friction
Ψ, Φ: Three-dimensional stream functions defined by Eq. (2.9)
$(\ )^*$: Dimensional quantity
$(\ )_e$: Inviscid edge condition at the body surface
$(\ )_i$: Injected gas
$(\ )_f$, $(\ )_\infty$: Freestream condition
$(\ )_r$: Reference condition
$(\ )_w$: Wall condition
$(\ )_0$: Basic term of perturbations
$(\ )_n$: Perturbation term

1. Introduction

One of the problems arising from high speed flight of the vehicles is the aerodynamic heating. At high Reynolds Number conditions, the analysis of such a problem should essentially be made using Prandtl's boundary layer approximation. For a lifting body in particular, the boundary layer is generally three-dimensional. Additionally it is pointed out that a small three-dimensional effect in the inviscid flow can cause a large effect in the boundary layer [1]. Hence a knowledge of the full three-dimensional boundary layer properties is necessary for a correct estimate of the local heat transfer and skin friction.

The high speed flow over a sharp conical body at angles of attack represents a three-dimensional fluid dynamic problem, encompassing a wide variety of phenomena.

The boundary layer on the conical body provides a practical example thereof, and leads to useful insights into the nature of more general three-dimensional boundary layer. Studies of the laminar boundary layer without mass injection on the conical body, especially a circular cone at angles of attack, have been made by a number of researchers. A major early paper was written by Moore. Moore [*2*] published a solution to similar boundary layer equations for very small angles of attack using small perturbation method, corresponding to Stone's perturbation solution for the inviscid conical flow. In another paper [*3*], Moore solved the similar boundary layer equations along the windward and leeward line of symmetry for small to moderate angles of attack. After the early work of Moore, progress on understanding the flow over the conical body was very slow, because of the lack of adequate method of solving boundary layer equations. However, the recent development of digital computers has made it possible to solve the full boundary layer equations numerically. A number of solutions of the boundary layer equations for the circular cone have been obtained by streamwise numerical integration, incorporating a wind-to-leeplane marching procedure at each streamwise location. The numerical methods are of great advantage to the cases of moderate to large angles of attack. However, these methods have the complex marching procedure. For the noncircular cone in particular, these methods become less desirable because of requring the initial profiles on the windward surface for the marching procedure, which is not readily obtainable. Moreover, solutions obtained by the numerical methods are not general in the sense that these depend closely on flow parameters (i.e., freestream Mach Number, wall temperature, body shape, etc.). To date, there are no general solutions to the equations of the three-dimensional boundary layer on the conical body.

The governing partial differential equations of the three-dimensional boundary layer are complex because of many flow parameters included. Moreover, at re-entry velocities, the thermal decomposition of protective heat shield introduces a significant quantity of foreign material into flowfield, further complicating the boundary layer analysis. Because of the complexities of the fully three-dimensional flow, most boundary layer analyses have been devoted to two-dimensional or axially symmetric flows. For the circular cone at angles of attack, many analyses [*4*]–[*9*] are available for estimating the influence of mass injectionon on boundary layer characteristics for axisymmetric or stagnation point flowfields. However, there are scarecely any analyses dealing with the influence of mass injection on fully three-dimensional boundary layer characteristics. There are no exact solutions, given in the form independent of flow parameters, to the equations of the three-dimensional, binary mixture boundary layer on the conical body. The binary mixture may take place under the condition of foreign gas injection into the boundary layer.

The purpose of the present paper is two-fold: first, to present the exact solution, given in the form independent of flow parameters, to the equations of the laminar boundary layer with and without mass injection on the conical body of arbitrary cross-section; second, to analyze the effects of mass injection on the boundary layer characteristics. Attension is especially directed toward estimating the mutual in-

fluence of mass injection and the cross-flow (or "secondary flow") on the local heat transfer and skin friction. For this purpose, the over-all flowfield will be solved using the small perturbation method. We shall deal with the conical body of which the cross-section is nearly circular but otherwise arbitrary. The boundary layer is assumed to be similar under the condition that the outer inviscid flow is conical, so that the injected mass flux rate is inversely proportional to the square root of the meridional distance from the body apex.

Chapter 2 gives the basic equations of the boundary layer. The familiar, binary mixture, three-dimensional boundary layer equations are transformed into similarity form. The present procedure of transformation is the extension of Moore's for the single gas case to the binary mixture case. In chapter 3, the over-all flowfield is solved. The outer inviscid conical flow solution is determined by the extension of Stone's perturbation solution for the circular cone. The exact first order perturbation solution of similar boundary layer equations is obtained in the general form, corresponding to the inviscid solution. In chapter 4, the Present theory is applied to the cases of several shapes of nonaxisymmetric conical bodies. At first, in order to check the validity of the present theoretical approach, solutions are compared with experimental data as well as those calculated by existing numerical method for the circular cone without mass injection. Next, the effects of mass injection (air-to-air, or helium-to-air) on the boundary layer characteristics are discussed in detail.

2. Boundary Layer Equations

In this investigation, the following assumptions are imposed on the flowfield: (1) The boundary layer is laminar and similar, and its thickness is very small compared with the body radius, (2) The outer inviscid flow has conical symmetry, (3) Constant Prandtl Number P_r, Schmidt Number S_c, and Chapman-Rubesin Number N, (4) Constant physical properties of each gas in the case of binary mixture, (5) No chemical reaction, radiation, ionization and dissociation in the boundary layer.

Since the present paper is concerned with small deformation from the basic circular cone and corresponding small departures of the entire flow from that occuring at basic axisymmetric flow condition, it will be convenient to refer all physical properties to the basic inviscid flow conditions at basic circular cone surface. The variables are normalized using reference conditions mentioned above as follows:

$$\left.\begin{array}{llll} u=u^*/u_r^*, & v=v^*/u_r^*, & w=w^*/u_r^*, & a=a^*/u_r^* \\ \rho=\rho^*/\rho_r^*, & p=p^*/(\rho_r^* u_r^{*2}), & T=T^*/(u_r^{*2}/2c_{pr}^*) & \\ h=h^*/u_r^{*2}, & \mu=\mu^*/\mu_r^*, & c_p=c_p^*/c_{pr}^* & \\ x=x^*/l_l^*, & y=y^*/l_l^*, & (l_l^*=\mu^*/(\rho_r^* u_r^*)) & \end{array}\right\} \tag{2.1}$$

2.1 *Basic equations*

The steady boundary layer equations in the boundary layer coordinate system

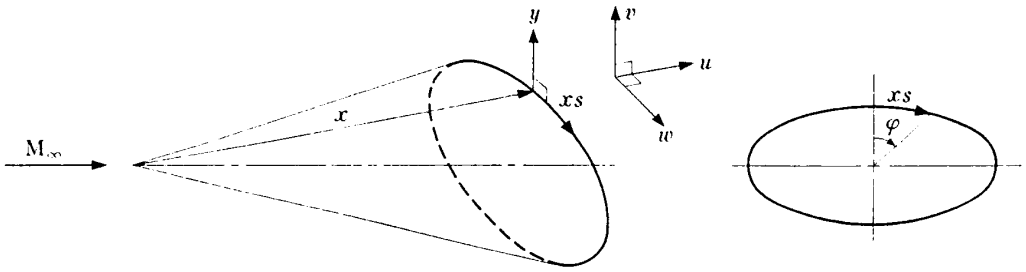

FIG. 1. Boundary layer coordinate system

shown in Fig. 1 may be written as follows:

$$\frac{\partial}{\partial x}(\rho x u)+\frac{\partial}{\partial y}(\rho x v)+\frac{1}{x}\frac{\partial}{\partial s}(\rho x w)=0 \tag{2.2}$$

$$\rho\left(u\frac{\partial u}{\partial x}+v\frac{\partial u}{\partial y}+\frac{w}{x}\frac{\partial u}{\partial s}-\frac{w^2}{x}\right)=-\frac{\partial p}{\partial x}+\frac{\partial}{\partial y}\left(\mu\frac{\partial u}{\partial y}\right) \tag{2.3}$$

$$\rho\left(u\frac{\partial w}{\partial x}+v\frac{\partial w}{\partial y}+\frac{w}{x}\frac{\partial w}{\partial s}+\frac{uw}{x}\right)=-\frac{1}{x}\frac{\partial p}{\partial s}+\frac{\partial}{\partial y}\left(\mu\frac{\partial w}{\partial y}\right) \tag{2.4}$$

$$\rho\left(u\frac{\partial c_i}{\partial x}+v\frac{\partial c_i}{\partial y}+\frac{w}{x}\frac{\partial c_i}{\partial s}\right)=\frac{\partial}{\partial y}\left(\frac{\mu}{S_c}\frac{\partial c_i}{\partial y}\right) \tag{2.5}$$

$$\begin{aligned}\rho c_p\left(u\frac{\partial T}{\partial x}+v\frac{\partial T}{\partial y}+\frac{w}{x}\frac{\partial T}{\partial s}\right)&=2u\frac{\partial p}{\partial x}+2\frac{w}{x}\frac{\partial p}{\partial s}\\&+2\mu\left[\left(\frac{\partial u}{\partial y}\right)^2+\left(\frac{\partial w}{\partial y}\right)^2\right]+\frac{\partial}{\partial y}\left(\frac{c_p\mu}{P_r}\frac{\partial T}{\partial y}\right)+\frac{\beta_1\mu}{S_c}\frac{\partial c_i}{\partial y}\frac{\partial T}{\partial y}\end{aligned} \tag{2.6}$$

where

$$c_i=\frac{\rho_i}{\rho},\quad S_c=\frac{\mu^*}{\rho^* D_{if}^*},\quad P_r=\frac{c_p^*\mu^*}{k^*},\quad \beta_1=\frac{c_{pi}^*-c_{pf}^*}{c_{pr}^*}=c_{pi}-1 \tag{2.7}$$

With foundamental thermodynamic relations of the perfect gas,

$$c_p=1+\beta_1 c_i,\quad \frac{1}{\rho}=\frac{\gamma-1}{2\gamma}\frac{T}{p}(1+\beta_2 c_i),\quad \beta_2=\frac{M_f^*}{M_i^*}-1 \tag{2.8}$$

Eqs. (2.2)–(2.6) can be simplified by making following transformations in turn. First of all, stream functions Ψ and Φ are introduced as:

$$\rho x u=\frac{\partial \Psi}{\partial y},\quad \rho x v=-\frac{\partial \Psi}{\partial x}-\frac{1}{x}\frac{\partial \Phi}{\partial s},\quad \rho x w=\frac{\partial \Phi}{\partial y} \tag{2.9}$$

(a) The Mangler transformation (to reduce the effect of x):

$$\hat{x}=L^2\int_0^x x^2dx=\frac{1}{3}L^2x^3,\quad \hat{y}=Lxy,\quad \hat{s}=s,\quad \hat{\Psi}=L\Psi,\quad \hat{\Phi}=L\Phi \tag{2.10}$$

(b) The Dorodnitsyn-Howarth transformation (to remove explicit dependence on the density):

$$X=\hat{x},\quad Y=\int_0^{\hat{y}}\rho dy,\quad Z=\hat{s},\quad F=\hat{\Psi},\quad G=\hat{\Phi} \tag{2.11}$$

(c) The Blasius transformation (to reduce the number of independent variables from three to two):

$$\lambda=X^{-1/2}Y,\quad \zeta=Z,\quad f=X^{-1/2}F,\quad g=X^{-1/2}G \tag{2.12}$$

The Blasius transformation is introduced under the condition that the outer inviscid flow is conical, that is, $\partial p/\partial x=0$. Application of the above transformation to Eqs. (2.2)–(2.6) produces the following:

$$\left(\frac{1}{2}f+\frac{1}{3}g_\zeta\right)f_{\lambda\lambda}-\frac{1}{3}g_\lambda f_{\lambda\zeta}+\frac{1}{3}(g_\lambda)^2+[Nf_{\lambda\lambda}]_\lambda=0 \tag{2.13}$$

$$\left(\frac{1}{2}f+\frac{1}{3}g_\zeta\right)g_{\lambda\lambda}-\frac{1}{3}g_\lambda g_{\lambda\zeta}-\frac{1}{3}f_\lambda g_\lambda-\frac{1}{3}\frac{p'(\zeta)}{\rho}+[Ng_{\lambda\lambda}]_\lambda=0 \tag{2.14}$$

$$\left(\frac{1}{2}f+\frac{1}{3}g_\zeta\right)c_{i,\lambda}-\frac{1}{3}g_\lambda c_{i,\lambda}+\left[\frac{N}{S_c}c_{i,\lambda}\right]_\lambda=0 \tag{2.15}$$

$$\begin{aligned}&\left(\frac{1}{2}f+\frac{1}{3}g_\zeta\right)c_pT_\lambda-\frac{1}{3}g_\lambda c_pT_\zeta+\frac{2}{3}\frac{p'(\zeta)}{\rho}g_\lambda\\&\quad+2N[(f_{\lambda\lambda})^2+(g_{\lambda\lambda})^2]+\left[\frac{N}{P_\lambda}c_pT_\lambda\right]_\lambda+\beta_1\frac{N}{S_c}c_{i,\lambda}T_\lambda=0\end{aligned} \tag{2.16}$$

and

$$N=\rho\mu,\quad u=f_\lambda,\quad w=g_\lambda \tag{2.17}$$

$$\rho v=-\sqrt{\frac{3}{x}}\left\{\frac{1}{2}(f-\lambda f_\lambda)+\frac{1}{3}g_\zeta+X^{1/2}Y_{\pm}f_\lambda+\frac{1}{3}X^{-1/2}g_\lambda(1+\rho\hat{y})\right\} \tag{2.18}$$

2.2 Boundary conditions

At the body surface: The cone surface is assumed to be isothermal. At the cone surface the temperature of the injected gas is equal to that of the wall; $T(0,\zeta)=T_w$. The usual no-slip condition for the tangential velocity components is imposed, so we put $u_w=f_\lambda(0,\zeta)=0$ and $w_w=g_\lambda(0,\zeta)=0$. As for mass injection rate, from Eq. (2.18),

$$(\rho v)_w=-\sqrt{\frac{3}{x}}\left[\frac{1}{2}f(0,\zeta)+\frac{1}{3}g_\zeta(0,\zeta)\right] \tag{2.19}$$

Under the assumption of the similar boundary layer the distribution of injection mass flux $(\rho v)_w$ is imposed to be inversely proportional to the square root of the meridional distance from the cone apex, that is, $(\rho v)_w \sim 1/\sqrt{x}$. The injection mass flux $(\rho v)_w$ may be determined by giving negative value to $[f(0,\zeta)/2+g_\zeta(0,\zeta)/3]$ in Eq. (2.19), or more simply by putting $f(0,\zeta)=f_w$ (f_w: injection rate parameter), and $g(0,\zeta)=0$ [9]. As for the concentration of the injected gas, the condition of zero net flux of the freestream gas, air, is imposed. Although other conditions are possible to treat mathematically, it was pointed out in Ref. [10] that zero net flux of the freestream gas at the surface is needed for a physically realistic solution from an aerodynamic point of view. This condition is given as

$$\left[\frac{N}{S_c}c_{i,\lambda}\right]_w=(1-c_{iw})\cdot\frac{1}{2}f_w \tag{2.20}$$

At the outer edge: At the outer edge of the boundary layer, u, w and T should take on the corresponding inviscid values. It is assumed that the particles of the injected gas do not reach the inviscid region, then we put $c_i(\infty,\zeta)=0$.

3. Perturbation Analysis

3.1. *Method of perturbation*

A solution to the boundary layer equations is sought as a perturbation of the basic axisymmetric flow which is formed around the circular cone with the same cross-sectional area as the conical body considered.

The conical body may be expressed in the wind-fixed polar coordinate system in Fig. 2 in the form

$$\theta=\theta_b(\varphi)=\bar{\theta}_b+\sum_n(\varepsilon_n\cos n\varphi+E_n\sin n\varphi) \tag{3.1}$$

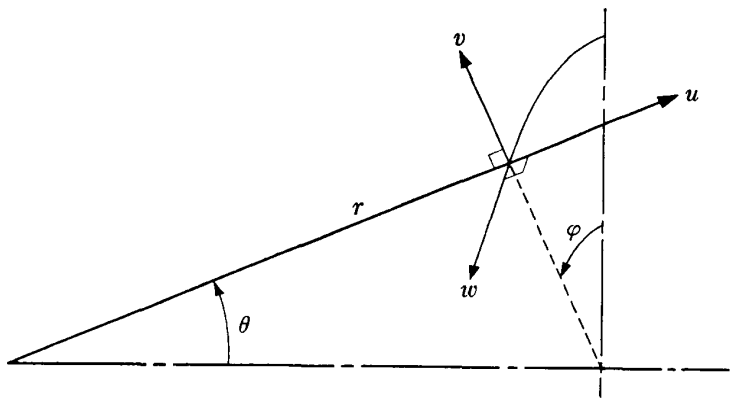

Fig. 2. Polar coordinate system

In this paper we deals with the conical bodies with nearly circular cross-section and with the case of small angles of attack. We assume

$$|n\varepsilon_n/\bar{\theta}_b|, \quad |nE_n/\bar{\theta}_b|, \quad |\alpha/\bar{\theta}_b| \ll 1 \tag{3.2}$$

Hereafter the order of magnitude of the above will be refered to $O(\varepsilon)$. In the perturbation analysis, we consider up to the first order in ε, and neglect the higher order. In the case of small angles of attack, i.e., $\alpha/\bar{\theta}_b = O(\varepsilon)$, the effect of the angles of attack may be contained in the term ε_1. For example, a $\bar{\theta}_b$-semi-apex circular cone immersed in the flow at the angle of attack can be expressed by

$$\theta = \theta_b(\varphi) = \bar{\theta}_b + \alpha \cos\varphi \qquad (\varepsilon_1 = \alpha) \tag{3.3}$$

If the conical body is expressed by Eq. (3.1), the $\bar{\theta}_b$ circular cone has the same cross-sectional area as the conical body considered. We shall refer to this circular cone as a basic circular cone.

We adopt the axisymmetric flow around this basic circular cone as a basic flow. The flow around the conical body expressed by Eq. (3.1) may be regarded to be perturbed from the basic flow by the small deformation from the basic circular cone.

For the conical body written in (r, θ, φ) system, it is convenient to rewrite the basic equations into (λ, φ) system. Relation between ζ and φ is, on neglecting $O(\varepsilon^2)$,

$$\frac{\partial}{\partial\zeta} = \frac{1}{\sin\bar{\theta}_b}\left\{1 - \cot\bar{\theta}_b \sum_n (\varepsilon_n \cos n\varphi + E_n \sin n\varphi)\right\}\frac{\partial}{\partial\varphi} \tag{3.4}$$

With Eq. (3.4), basic equations (2.13)–(2.16) and boundary conditions become

$$\left(\frac{1}{2}f + \frac{1}{3\sin\bar{\theta}_b}g_\varphi\right)f_{\lambda\lambda} - \frac{1}{3\sin\bar{\theta}_b}g_\lambda f_{\lambda\varphi} + \frac{1}{3}(g_\lambda)^2 + Nf_{\lambda\lambda\lambda} = 0 \tag{3.5}$$

$$\begin{aligned}\left(\frac{1}{2}f + \frac{1}{3\sin\bar{\theta}_b}g_\varphi\right)g_{\lambda\lambda} - \frac{1}{3\sin\bar{\theta}_b}g_\lambda g_{\lambda\varphi} \\ - \frac{1}{3}f_\lambda g_\lambda - \frac{1}{3\sin\bar{\theta}_b}\frac{p'(\varphi)}{\rho} + Ng_{\lambda\lambda\lambda} = 0\end{aligned} \tag{3.6}$$

$$\left(\frac{1}{2}f + \frac{1}{3\sin\bar{\theta}_b}g_\varphi\right)c_{i,\lambda} - \frac{1}{3\sin\bar{\theta}_b}g_\lambda c_{i,\varphi} + \frac{N}{S_c}c_{i,\lambda\lambda} = 0 \tag{3.7}$$

$$\begin{aligned}\left(\frac{1}{2}f + \frac{1}{3\sin\bar{\theta}_b}g_\varphi\right)c_p T_\lambda - \frac{1}{3\sin\bar{\theta}_b}g_\lambda c_p T_\varphi \\ + \frac{2}{3\sin\bar{\theta}_b}\frac{p'(\varphi)}{\rho}g_\lambda + 2N[(f_{\lambda\lambda})^2 + (g_{\lambda\lambda})^2] \\ + \frac{N}{P_r}[c_p T_\lambda]_\lambda + \beta_1\frac{N}{S_c}c_{i,\lambda}T_\lambda = 0\end{aligned} \tag{3.8}$$

Boundary conditions

$$\left.\begin{aligned}&f(0,\varphi) = f_w, \quad f_\lambda(0,\varphi) = 0, \quad g(0,\varphi) = g_\lambda(0,\varphi) = 0 \\ &\frac{N}{S_c}c_{i,\lambda}(0,\varphi) = [1 - c_i(0,\varphi)]\cdot\frac{1}{2}f_w, \quad T(0,\varphi) = T_w\end{aligned}\right\} \tag{3.9}$$

$$\left.\begin{aligned} f_i(\infty, \varphi) &= u_e(\varphi), \quad g_i(\infty, \varphi) = w_e(\varphi) \\ c_i(\infty, \varphi) &= 0, \quad T(\infty, \varphi) = T_e(\varphi) \end{aligned}\right\}$$

3.2 *Inviscid conical flow solution—outer edge conditions*

In order to solve the boundary layer equations, one must have values for the inviscid velocities and temperature at the surface of the body. These values will serve as boundary conditions at the outer edge of the boundary layer, and also determine the pressure gradients in the flow. Many authors [*11*]–[*14*] have treated the subject of inviscid conical flow, especially for the case of the circular cone. The Stone's perturbation solution for the circular cone at small angles of attack is the simplest, analytic one [*11*]. In this paper, we use the solution in Ref. [*9*] as the outer edge conditions, which is the extension of Stone's to the cases of nonaxisymmetric conical bodies expressed by Eq. (3.1). This is the first order perturbation solution, and is essentially the same one as given in Ref. [*14*]. Here we give only a brief description. In this section, normalization is made in the same manner as previous section, but for the analytical convenience, the freestream reservoir condition and a limiting velocity are used as the reference conditions. The normalized governing equations of the inviscid conical flow may be written in the polar coordinate system (Fig. 2) as:

$$\frac{\partial}{\partial\theta}(\rho v \sin\theta) + \frac{\partial}{\partial\varphi}(\rho w) + 2\rho u \sin\theta = 0 \tag{3.10}$$

$$u\frac{\partial u}{\partial\theta} + \frac{w}{\sin\theta}\frac{\partial u}{\partial\varphi} - v^2 - w^2 = 0 \tag{3.11}$$

$$v\frac{\partial v}{\partial\theta} + \frac{w}{\sin\theta}\frac{\partial v}{\partial\varphi} + \frac{1}{\rho}\frac{\partial p}{\partial\theta} + uv - w^2\cot\theta = 0 \tag{3.12}$$

$$v\frac{\partial w}{\partial\theta} + \frac{w}{\sin\theta}\frac{\partial w}{\partial\varphi} + \frac{1}{\rho\sin\theta}\frac{\partial p}{\partial\varphi} + uw + vw\cot\theta = 0 \tag{3.13}$$

$$\frac{2}{\gamma-1}a^2 + u^2 + v^2 + w^2 = 2h + u^2 + v^2 + w^2 = 1 \tag{3.14}$$

$$a^2 = \frac{\gamma p}{\rho} \tag{3.15}$$

where a and h are speed of sound and static enthalpy, respectively. Combining Eqs. (3.10)–(3.15) results in

$$\begin{aligned} &u\left(2 - \frac{v^2+w^2}{a^2}\right) + v\cot\theta + \frac{\partial v}{\partial\theta}\left(1 - \frac{v^2}{a^2}\right) \\ &\quad + \frac{1}{\sin\theta}\frac{\partial w}{\partial\varphi}\left(1 - \frac{w^2}{a^2}\right) - \frac{vw}{a^2}\left(\frac{1}{\sin\theta}\frac{\partial w}{\partial\varphi} + \frac{\partial w}{\partial\theta}\right) = 0 \end{aligned} \tag{3.16}$$

The flowfield is assumed to be represented as the sum of the basic axisymmetric field

around the basic circular cone and correction perturbed terms due to the deformation from the basic circular cone, such as:

$$u(\theta, \varphi)=\bar{u}(\theta)+\sum_n (\varepsilon_n u_n(\theta) \cos n\varphi + E_n U_n(\theta) \sin n\varphi) \tag{3.17}$$

$$v(\theta, \varphi)=\bar{v}(\theta)+\sum_n (\varepsilon_n v_n(\theta) \cos n\varphi + E_n V_n(\theta) \sin n\varphi) \tag{3.18}$$

$$w(\theta, \varphi)=\sum_n (\varepsilon_n w_n(\theta) \sin n\varphi - E_n W_n(\theta) \cos n\varphi) \tag{3.19}$$

$$p(\theta, \varphi)=\bar{p}(\theta)+\sum_n (\varepsilon_n p_n(\theta) \cos n\varphi + E_n P_n(\theta) \sin n\varphi) \tag{3.20}$$

$$\rho(\theta, \varphi)=\bar{\rho}(\theta)+\sum_n (\varepsilon_n \rho_n(\theta) \cos n\varphi + E_n R_n(\theta) \sin n\varphi) \tag{3.21}$$

$$h(\theta, \varphi)=\bar{h}(\theta)+\sum_n (\varepsilon_n h_n(\theta) \cos n\varphi + E_n H_n(\theta) \sin n\varphi) \tag{3.22}$$

Here zeroth order terms, denoted by $\bar{(\ )}$, correspond to the familiar Taylor-Maccoll solution [*15*]. Substituting Eqs. (3.17)–(3.22) into Eqs. (3.10)–(3.16) and equating the sum of terms of unit order and the sum of terms of first order in ε_n, E_n, to zero separately give differential equations for the unknowns: $\bar{u}(\theta)$, $u_n(\theta)$, $\cdots$, $H_n(\theta)$.

If the conical shock shape is assumed to be

$$\theta=\theta_s(\varphi)=\bar{\theta}_s+\sum_n (\varepsilon_n \theta_{sn} \cos n\varphi + E_n \Theta_{sn} \sin n\varphi) \tag{3.23}$$

then, Rankin-Hugoniot relations at the shock wave and the tangency condition at the body surface yield boundary conditions stated at $\theta=\bar{\theta}_s$ and $\theta=\bar{\theta}_b$, respectively, which result from Taylor series expansions about the points $\bar{\theta}_s$ and $\bar{\theta}_b$.

Consequently, the inviscid edge properties may be written in the following form (again corresponding to reference conditions of previous section):

$$u_e(\varphi)=1+\sum_n (\varepsilon_n u_{en} \cos n\varphi + E_n U_{en} \sin n\varphi) \tag{3.24}$$

$$w_e(\varphi)=\sum_n (\varepsilon_n w_{en} \sin n\varphi - E_n W_{en} \cos n\varphi) \tag{3.25}$$

$$p_e(\varphi)=\bar{p}_e+\sum_n (\varepsilon_n p_{en} \cos n\varphi + E_n P_{en} \sin n\varphi) \tag{3.26}$$

$$T_e(\varphi)=\bar{t}_e+\sum_n (\varepsilon_n(-2u_{en}) \cos n\varphi + E_n(-2U_{en}) \sin n\varphi) \tag{3.27}$$

3.3 Perturbation equations of the boundary layer

With the assumption that the entire flow may be represented as the sum of the basic axisymmetric flow and correction perturbed term, $f(\lambda, \varphi)$, $g(\lambda, \varphi)$, $c_i(\lambda, \varphi)$ and $T(\lambda, \varphi)$ may be written in a form chosen to be consistent with the relation (3.24)–(3.27) to be imposed as outer edge boundary conditions

$$f(\lambda, \varphi)=f_0(\lambda)+\sum_n \{\varepsilon_n u_{en} f_n(\lambda) \cos n\varphi + E_n U_{en} F_n(\lambda) \sin n\varphi\} \tag{3.28}$$

$$g(\lambda, \varphi)=\sum_n \{\varepsilon_n w_{en} g_n(\lambda) \sin n\varphi - E_n W_{en} G_n(\lambda) \cos n\varphi\} \tag{3.29}$$

$$c_i(\lambda, \varphi)=c_{i0}(\lambda)+\sum_n \{\varepsilon_n u_{en} c_{in}(\lambda) \cos n\varphi + E_n U_{en} C_{in}(\lambda) \sin n\varphi\} \tag{3.30}$$

$$T(\lambda, \varphi)=t_0(\lambda)+\sum_n \{\varepsilon_n(-2u_{en}) t_n(\lambda) \cos n\varphi + E_n(-2U_{en}) T_n(\lambda) \sin n\varphi\} \tag{3.31}$$

The specific heat at constant pressure may be expressed in perturbation form with the aid of Eqs. (2.8) and (3.30):

$$c_p(\lambda, \varphi)=c_{p0}(\lambda, \varphi)+\sum_n (\varepsilon_n c_{pn}(\lambda) \cos n\varphi + E_n C_{pn}(\lambda) \sin n\varphi) \tag{3.32}$$

where,

$$c_{p0}(\lambda)=1+\beta_1 c_{i0}(\lambda), \quad c_{pn}(\lambda)=u_{en}\beta_1 c_{in}(\lambda), \quad C_{pn}(\lambda)=U_{en}\beta_1 C_{in}(\lambda) \tag{3.33}$$

Substituting Eqs. (3.28)–(3.31) into Eqs. (3.5)–(3.8) and into the boundary conditions Eq. (3.9), and equating the sum of terms of unit order and the sum of first order in ε_n to zero separately yield following ordinary differential equations and boundary conditions:

Zeroth order,

$$f_0 f_0'' + 2N f_0''' = 0 \tag{3.34}$$

$$f_0 c_{i0}' + 2\frac{N}{S_c} c_{i0}'' = 0 \tag{3.35}$$

$$\frac{N}{P_r} c_{p0} t_0'' + B t_0' + 2N(f_0'')^2 = 0 \tag{3.36}$$

where

$$B=\frac{1}{2} f_0 c_{p0} + \beta_1\left(\frac{N}{P_r}+\frac{N}{S_c}\right) c_{i0}' \tag{3.37}$$

First order in ε_n, $(n=1, 2, 3, \cdots)$,

$$f_0'' f_n + f_0 f_n'' + 2N f_n''' + \left(\frac{2n}{3 \sin \bar{\theta}_b} \frac{w_{en}}{u_{en}}\right) f_0'' g_n = 0 \tag{3.38}$$

$$3 f_0 g_n'' - 2 f_0' g_n' + 6N g_n''' + \frac{2}{\bar{t}_e} t_0(1+\beta_2 c_{i0}) = 0 \tag{3.39}$$

$$f_0 c_{in}' + 2\frac{N}{S_c} c_{in}'' + \left[f_n + \left(\frac{2n}{3 \sin \bar{\theta}_b} \frac{w_{en}}{u_{en}}\right) g_n\right] c_{i0}' = 0 \tag{3.40}$$

$$\begin{aligned} &\frac{N}{P_r} c_{p0} t_n'' + B t_n' - \left[\frac{1}{2}\beta_1\left(\frac{1}{2} f_0 t_0' + \frac{N}{P_r} t_0''\right) c_{in} + \frac{1}{2}\beta_1\left(\frac{N}{P_r}+\frac{N}{S_c}\right) t_0' c_{in}'\right. \\ &\left. + \frac{1}{4} c_{p0} t_0' \left\{f_n + \left(\frac{2n}{3 \sin \bar{\theta}_b} \frac{w_{en}}{u_{en}}\right) g_n\right\} + 2N f_0'' f_n''\right] = 0 \end{aligned} \tag{3.41}$$

Boundary conditions

$$\left.\begin{aligned} &f_0(0)=f_w, \quad f_0'(0)=0, \quad f_0'(\infty)=1 \\ &c_{i0}'(0)=[1-c_{i0}(0)]\frac{S_c}{N}\cdot\frac{1}{2}f_w, \qquad c_{i0}(\infty)=0 \\ &t_0(0)=T_w, \qquad t_0(\infty)=\bar{t}_e \end{aligned}\right\} \tag{3.42}$$

$$\left.\begin{aligned} &f_n(0)=f_n'(0)=0, \qquad f_n'(\infty)=1 \\ &g_n(0)=g_n'(0)=0 \qquad g_n'(\infty)=1 \\ &c_{in}'(0)=-c_{in}(0)\frac{S_c}{N}\cdot\frac{1}{2}f_w, \qquad c_{in}(\infty)=0 \\ &t_n(0)=0, \qquad t_n(\infty)=1 \end{aligned}\right\} \tag{3.43}$$

together with same equations with capital letters (F_n, G_n, etc.) replacing the small letters (f_n, g_n, etc.) throughout. Here the primes denote differentiation with respect to the similarity variable λ.

3.4. *Solution of perturbation equations*

The flow parameters (T_w, $\bar{t}_e$, u_{en}, w_{en}, $\bar{\theta}_b$ and n) appearing in Eqs. (3.38)–(3.42) depend on the problem. It is necessary to eliminate these flow parameters in the solution in order to obtain the general solution. The functions $f_0(\lambda)$ and $c_{i0}(\lambda)$ are independent of the flow parameters.

Letting

$$\left.\begin{aligned} &A_1=T_w-(\bar{t}_e+J_{01}(0)), \qquad A_2=\frac{1}{\bar{t}_e}, \qquad A_3=A_1A_2 \\ &A_4^n=\frac{2n}{3\sin\bar{\theta}_b}\frac{w_{en}}{u_{en}}, \qquad A_5^n=A_2A_4^n, \qquad A_6^n=A_3A_4^n \\ &A_7^n=A_1A_4^n, \qquad A_8^n=A_1A_3A_4^n \end{aligned}\right\} \tag{3.44}$$

then, the functions $t_0(\lambda)$, $f_n(\lambda)$, $g_n(\lambda)$, $c_{in}(\lambda)$ and $t_n(\lambda)$ may be expressed as linear combinations of functions not depending on flow parameters:

$$t_0(\lambda)=\frac{1}{A_2}+J_{01}(\lambda)+A_1J_{02}(\lambda) \tag{3.45}$$

$$f_n(\lambda)=J_{f1}(\lambda)+A_4^nJ_{f2}(\lambda)+A_5^nJ_{f3}(\lambda)+A_6^nJ_{f4}(\lambda) \tag{3.46}$$

$$g_n(\lambda)=J_{g1}(\lambda)+A_2J_{g2}(\lambda)+A_3J_{g3}(\lambda) \tag{3.47}$$

$$c_{in}(\lambda)=J_{c1}(\lambda)+A_4^nJ_{c2}(\lambda)+A_5^nJ_{c3}(\lambda)+A_6^nJ_{c4}(\lambda) \tag{3.48}$$

$$\begin{aligned} t_n(\lambda)=&J_{t1}(\lambda)+A_1J_{t2}(\lambda)+A_4^nJ_{t3}(\lambda)+A_5^nJ_{t4}(\lambda) \\ &+A_6^nJ_{t5}(\lambda)+A_7^nJ_{t6}(\lambda)+A_8^nJ_{t7}(\lambda) \end{aligned} \tag{3.49}$$

Here $J_{01}(\lambda)$, $J_{02}(\lambda)$, $\cdots$, $J_{t7}(\lambda)$ satisfy the following equations and boundary conditions:

$$\frac{N}{P_r}c_{p0}J''_{01}+BJ'_{01}+2N(f''_0)^2=0 \qquad (J'_{01}(0)=0,\ J_{01}(\infty)=0) \tag{3.50}$$

$$\frac{N}{P_r}c_{p0}J''_{02}+BJ'_{02}=0 \qquad (J_{02}(0)=1,\ J_{02}(\infty)=0) \tag{3.51}$$

$$f''_0J_{f1}+f_0J''_{f1}+2NJ'''_{f1}=0 \qquad (J_{f1}(0)=J'_{f1}(0)=0,\ J'_{f1}(\infty)=1) \tag{3.52}$$

$$f''_0J_{f2}+f_0J''_{f2}+2NJ'''_{f2}+f''_0J_{g1}=0 \qquad (J_{f2}(0)=J'_{f2}(0)=J'_{f2}(\infty)=0) \tag{3.53}$$

$$f''_0J_{f3}+f_0J''_{f3}+2NJ'''_{f3}+f''_0J_{g2}=0 \qquad (J_{f3}(0)=J'_{f3}(0)=J'_{f3}(\infty)=0) \tag{3.54}$$

$$f''_0J_{f4}+f_0J''_{f4}+2NJ'''_{f4}+f''_0J_{g3}=0 \qquad (J_{f4}(0)=J'_{f4}(0)=J'_{f4}(\infty)=0) \tag{3.55}$$

$$\begin{gathered}3f_0J''_{g1}-2f'_0J'_{g1}+6NJ'''_{g1}+2(1+\beta_2c_{i0})=0\\ (J_{g1}(0)=J'_{g1}(0)=0,\ J'_{g1}(\infty)=1)\end{gathered} \tag{3.56}$$

$$\begin{gathered}3f_0J''_{g2}-2f'_0J'_{g2}+6NJ'''_{g2}+2J_{01}(1+\beta_2c_{i0})=0\\ (J_{g2}(0)=J'_{g2}(0)=J'_{g2}(\infty)=0)\end{gathered} \tag{3.57}$$

$$\begin{gathered}3f_0J''_{g3}-2f'_0J'_{g3}+6NJ'''_{g3}+2J_{02}(1+\beta_2c_{i0})=0\\ (J_{g3}(0)=J'_{g3}(0)=J'_{g3}(\infty)=0)\end{gathered} \tag{3.58}$$

$$\begin{gathered}f_0J'_{c1}+2\frac{N}{S_c}J''_{c1}+c'_{i0}J_{f1}=0\\ \left(J'_{c1}(0)=-J_{c1}(0)\frac{S_c}{N}\frac{1}{2}f_w,\ J_{c1}(\infty)=0\right)\end{gathered} \tag{3.59}$$

$$\begin{gathered}f_0J'_{c1}+2\frac{N}{S_c}J''_{c2}+c'_{i0}(J_{f2}+J_{g1})=0\\ \left(J'_{c2}(0)=-J_{c2}(0)\frac{S_c}{N}\frac{1}{2}f_w,\ J_{c2}(\infty)=0\right)\end{gathered} \tag{3.60}$$

$$\begin{gathered}f_0J'_{c3}+2\frac{N}{S_c}J''_{c3}+c'_{i0}(J_{f3}+J_{g2})=0\\ \left(J'_{c3}(0)=-J_{c3}(0)\frac{S_c}{N}\frac{1}{2}f_w,\ J_{c3}(\infty)=0\right)\end{gathered} \tag{3.61}$$

$$\begin{gathered}f_0J'_{c4}+2\frac{N}{S_c}J''_{c4}+c'_{i0}(J_{f4}+J_{g3})=0\\ \left(J'_{c4}(0)=-J_{c4}(0)\frac{S_c}{N}\frac{1}{2}f_w,\ J_{c4}(\infty)=0\right)\end{gathered} \tag{3.62}$$

$$\frac{N}{P_r}c_{p0}J''_{t1}+BJ'_{t1}-\left[\frac{1}{2}\beta_1\left(\frac{1}{2}f_0J'_{01}+\frac{N}{P_r}J''_{01}\right)J_{c1}+\frac{1}{2}\beta_1\left(\frac{N}{P_r}+\frac{N}{S_c}\right)J'_{01}J'_{c1}+\frac{1}{4}c_{p0}J'_{01}J_{f1}+2Nf''_0J''_{f1}\right]=0 \tag{3.63}$$

$$(J_{t1}(0)=0,\ J_{t1}(\infty)=1)$$

$$\frac{N}{P_r}c_{p0}J''_{t2}+BJ'_{t2}-\left[\frac{1}{2}\beta_1\left(\frac{1}{2}f_0J'_{02}+\frac{N}{P_r}J''_{02}\right)J_{c1}+\frac{1}{2}\beta_1\left(\frac{N}{P_r}+\frac{N}{S_c}\right)J'_{02}J'_{c1}+\frac{1}{4}c_{p0}J'_{02}J_{f1}\right]=0 \tag{3.64}$$

$$(J_{t2}(0)=J_{t2}(\infty)=0)$$

$$\frac{N}{P_r}c_{p0}J''_{t3}+BJ'_{t3}-\left[\frac{1}{2}\beta_1\left(\frac{1}{2}f_0J'_{01}+\frac{N}{P_r}J'_{01}\right)J_{c2}+\frac{1}{2}\beta_1\left(\frac{N}{P_r}+\frac{N}{S_c}\right)J'_{01}J'_{c2}+\frac{1}{4}c_{p0}J'_{01}(J_{f2}+J_{g1})+2Nf''_0J''_{f2}\right]=0 \tag{3.65}$$

$$(J_{t3}(0)=J_{t3}(\infty)=0)$$

$$\frac{N}{P_r}c_{p0}J''_{t4}+BJ'_{t4}-\left[\frac{1}{2}\beta_1\left(\frac{1}{2}f_0J'_{01}+\frac{N}{P_r}J''_{01}\right)J_{c3}+\frac{1}{2}\beta_1\left(\frac{N}{P_r}+\frac{N}{S_c}\right)J'_{01}J'_{c3}+\frac{1}{4}c_{p0}J'_{01}(J_{f3}+J_{g2})+2Nf''_0J''_{f3}\right]=0 \tag{3.66}$$

$$(J_{t4}(0)=J_{t4}(\infty)=0)$$

$$\frac{N}{P_r}c_{p0}J''_{t5}+BJ'_{t5}-\left[\frac{1}{2}\beta_1\left(f_0J'_{01}+\frac{N}{P_r}J''_{01}\right)J_{c4}+\frac{1}{2}\beta_1\left(\frac{1}{2}f_0J'_{02}+\frac{N}{P_r}J''_{02}\right)J_{c3}+\frac{1}{2}\beta_1\left(\frac{N}{P_r}+\frac{N}{S_c}\right)(J'_{01}J'_{c4}+J'_{02}J'_{c3})+\frac{1}{4}c_{p0}\{J'_{01}(J_{f4}+J_{g3})+J'_{02}(J_{f3}+J_{g2})\}+2Nf''_0J''_{f4}\right]=0 \tag{3.67}$$

$$(J_{t5}(0)=J_{t5}(\infty)=0)$$

$$\frac{N}{P_r}c_{p0}J''_{t6}+BJ'_{t6}-\left[\frac{1}{2}\beta_1\left(\frac{1}{2}f_0J'_{02}+\frac{N}{P_r}J''_{02}\right)J_{c2}+\frac{1}{2}\beta_1\left(\frac{N}{P_r}+\frac{N}{S_c}\right)J'_{02}J'_{c2}+\frac{1}{4}c_{p0}J'_{02}(J_{f2}+J_{g1})\right]=0 \tag{3.68}$$

$$(J_{t6}(0)=J_{t6}(\infty)=0)$$

$$\frac{N}{P_r}c_{p0}J''_{t7}+BJ'_{t7}-\left[\frac{1}{2}\beta_1\left(\frac{1}{2}f_0J'_{02}+\frac{N}{P_r}J''_{02}\right)J_{c1}+\frac{1}{2}\beta_1\left(\frac{N}{P_r}+\frac{N}{S_c}\right)J'_{02}J'_{c4}+\frac{1}{4}c_{p0}J'_{02}(J_{f4}+J_{g3})\right]=0 \tag{3.69}$$

$$(J_{t7}(0)=J_{t7}(\infty)=0)$$

These differential equations and boundary conditions for the functions $J_{01}(\lambda), \cdots, J_{t7}(\lambda)$ can be solved once and for all, with no regard for the flow parameters of the problem.

3.5. *Boundary layer characteristics*

Local heat transfer and skin friction: Heat is transfered by means of conduction and diffusion. The local heat transfer at the surface may be written in the transformed form as:

$$q=-\sqrt{\frac{3}{x}}\left[\frac{N}{P_r}T_\lambda+\beta_1\left(\frac{N}{P_r}c_iT_\lambda+\frac{N}{S_c}Tc_{i,\lambda}\right)\right]_w \tag{3.70}$$

The meridional and circumferential components of the skin friction are given in the transformed form as:

$$\tau_x=[Nf_{\lambda\lambda}]_w, \qquad \tau_\varphi=[Ng_{\lambda\lambda}]_w \tag{3.71}$$

In order to show the effects of the mass injection and cross-flow, q and τ are normalized by $\tilde{q}_0$and $\tilde{\tau}_{x0}$, respectively in the figures. The quantities $\tilde{q}_0$ and $\tilde{\tau}_{x0}$ are the local heat transfer and skin friction in the case of the basic axisymmetic flow without mass injection.

Streamline: The streamline on the surface is determined by the differential equation: $(1/x\sin\theta)dx/d\varphi=u/w$. The inviscid streamline on the surface is $dx/d\varphi=x\sin\theta_b u_e/w_e$. The limiting streamline of the boundary layer is obtained by use of Eq. (2.17) and L'Hospital's rule,

$$\frac{dx}{d\varphi}=\lim_{y\to 0}\left(x\sin\theta\frac{u}{w}\right)=x\sin\theta_b\left[\frac{f_{\lambda\lambda}}{g_{\lambda\lambda}}\right]_w \tag{3.72}$$

4. Application—Results and Discussion

Results obtained with the previously derived solution are presented for the flow-fields around the several shapes of conical bodies with mass injection (air-to-air, or helium-to-air) at angles of attack immersed in supersonic freestream of Mach Numbers 5 and 10. Computational conditions for cases studied are as follows: The freestream is the air flow with a ratio of specific heats of 1.4; Prandtl Numbers are $P_r=0.738$ for air injection or no injection case and $P_r=0.743$ for helium injection case; In the case of helium injection Schmidt Number S_c is 0.834 and the ratio of constant pressure specific heats c_{pi}/c_{pf} is 5.18 and the ratio of molecular weights M_i^*/M_f^* is 1/7.25; Chapman-Rubesin Number N is unity for all cases studied.

In advance of the presentation of results, it is necessary to check the validity of the present theoretical approach. In doing so, the present solution is compared directly with experimental data as well as those calculated by existing numerical methods. The comparison of the surface pressure distribution for a 20° semi-apex circular cone is shown in Fig. 3, in which the small circles and the dashed line show

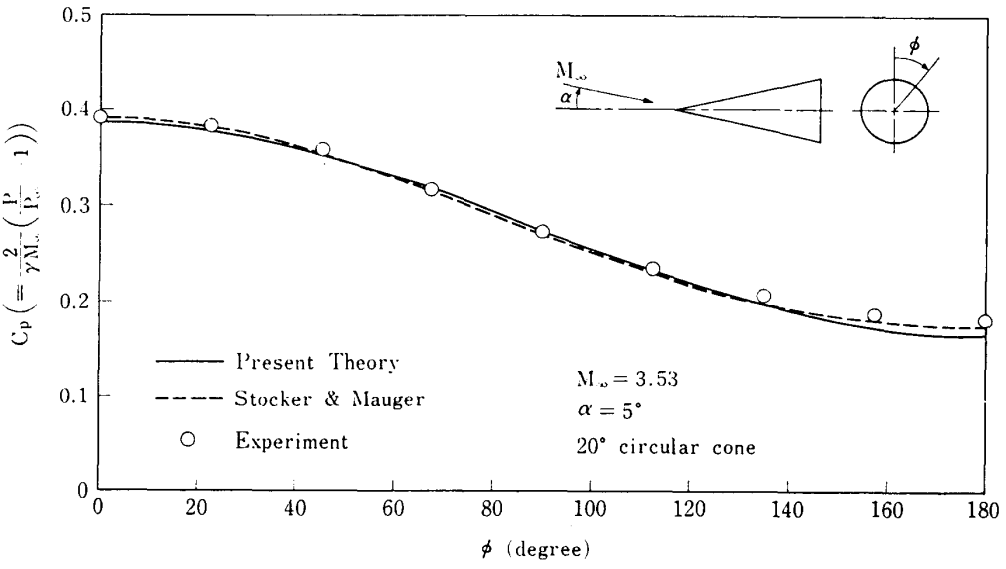

Fig. 3. Comparison of surface pressure distribution

experimental data from Ref. [*16*] and the result calculated using inverse method by Stocker and Mauger [*13*], respectively. The present result shows close agreement with experimental ones as well as with that of Stocker and Mauger. Only a few experimental studies are available of laminar boundary layer flow. Among these, Tracy's [*17*] provides valuable raw data which can be used as a basis for comparison with theoretical results, though it is for the case of no injection. Comparison of local heat transfer is shown in Fig. 4, in which the dashed line is the result of McGowan et al. [*18*] obtained by the wind-to-leeplane marching numerical integration of Moore's similar boundary layer equations. As can be seen with the figures, the present theoretical result agrees well with experimental one.

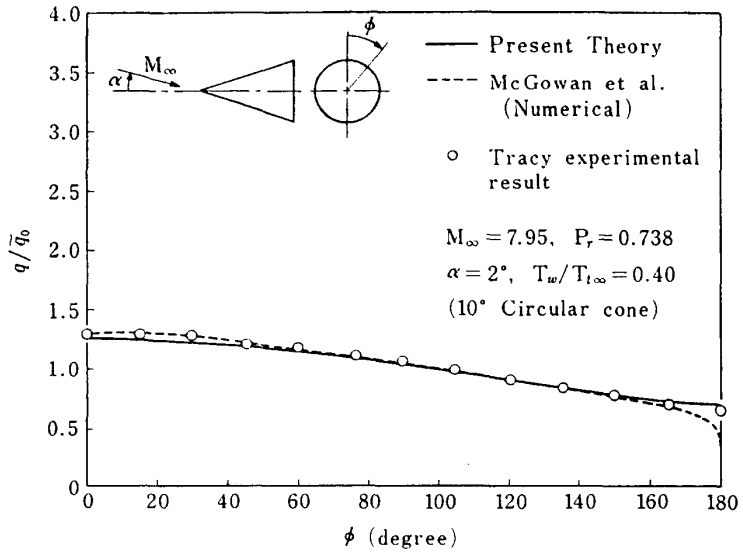

FIG. 4. Comparison of local heat transfer

Circular cone at angles of attack: The results for the case of the 10° circular cone at 2° angle of attack at $M_\infty = 5$ are summarized in Figs. 5–8. Fig. 5 shows limiting streamlines for air and helium injections. In the figure, the outer inviscid streamline and limiting stream lines for no injection case are also drawn. Since the inviscid flow about the circular cone at angles of attack is "conical", the pressure gradient at the outer edge of the boundary layer is entirely circumferential. Since the pressure tends to be constant across the boundary layer, the fluid in the boundary layer is subject to the same pressure gradient as is the outer flow, but less inertia with which to resist its effect, and thus it tends to follow the direction of the pressure gradient more closely than does the outer flow. Fig. 6 shows profiles of circum-

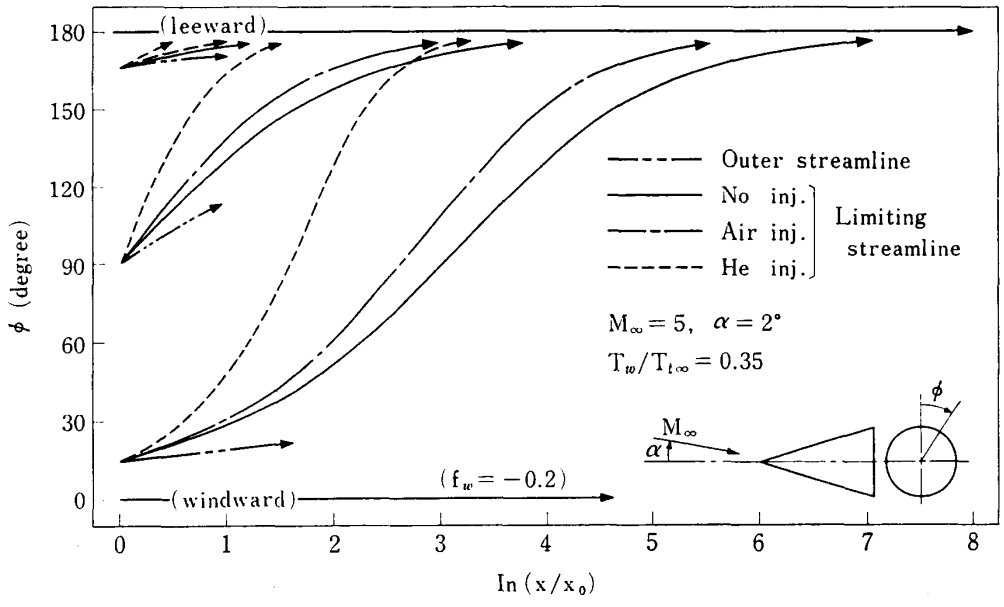

FIG. 5. Limiting streamlines for air and helium injections; 10° circular cone

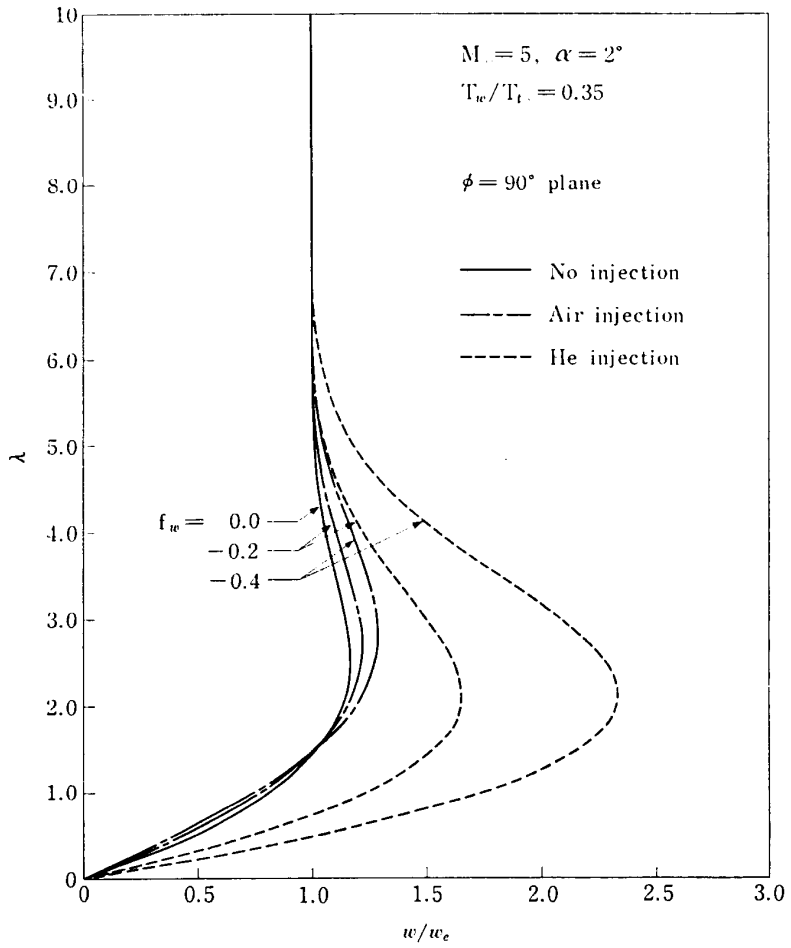

FIG. 6. Effect on mass injection on profiles of circumferential velocity component on $\phi=90°$ plane; 10° circular cone

ferential velocity component on $\phi=90°$ plane. It is seen that as mass injection rate increases the boundary layer thickness increases. In addition, maximum values of w/w_e also increase with increasing mass injection rate in order to satisfy the requirement of momentum conservation in the circumferential direction. As is seen with the figure, the maximum value of w/w_e is much greater in magnitude for helium injection than for air injection. Hence, the influence of helium injection on the boundary layer characteristics is more remarkable than is found in the case of air injection.

Fig. 7 shows the influence of mass injection on heat transfer. Heat is transported at the surface by two methods: conduction and diffusion (see Eq. (3.70)). Since the constant pressure specific heat of helium is large compared with that of air, the contribution of the diffusion to the heat transfer is larger than that of conduction. Hence, the reduction of heat transfer is more remarkable on the leeward side, on which the helium concentration becomes maximum, than on the windward side. Fig. 8 shows the influence of mass injection on skin friction. The effect of mass injection is to decrease skin friction. In the case of air injection, the circumferential skin friction hardly decreases with increasing mass injection. The circumferential skin

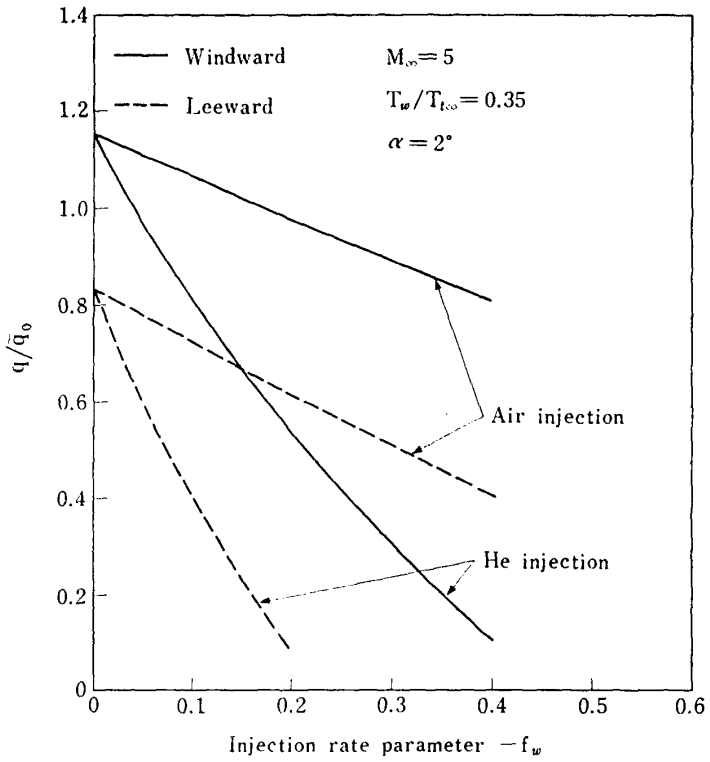

FIG. 7. Heat transfar on the symmetry plane vs. injection rate parameter; 10° circular cone

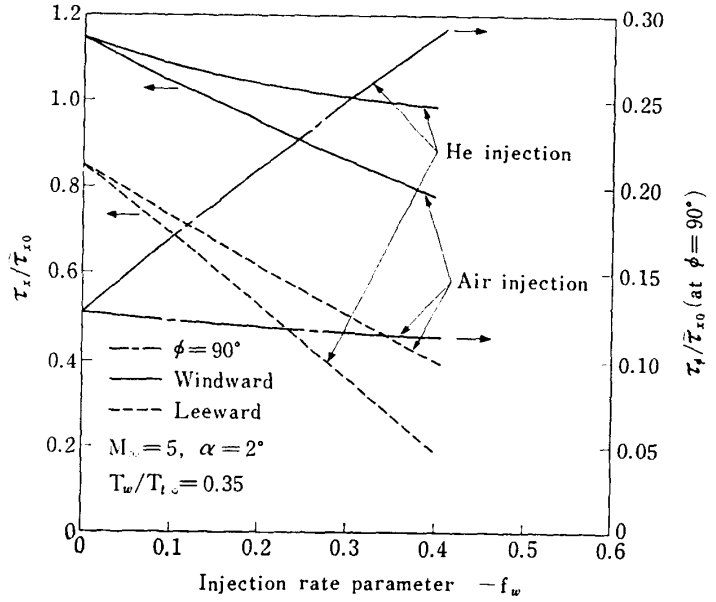

FIG. 8. Skin friction vs. injection rate parameter; 10° circular cone

friction, however, increases in the case of helium injection because of large increase of circumferential velocity component w due to mass injection.

Fig. 9 shows the influence of the variation in wall temperature on profiles of the circumferential velocity component for $f_w = -0.25$. It is seen that as wall temper-

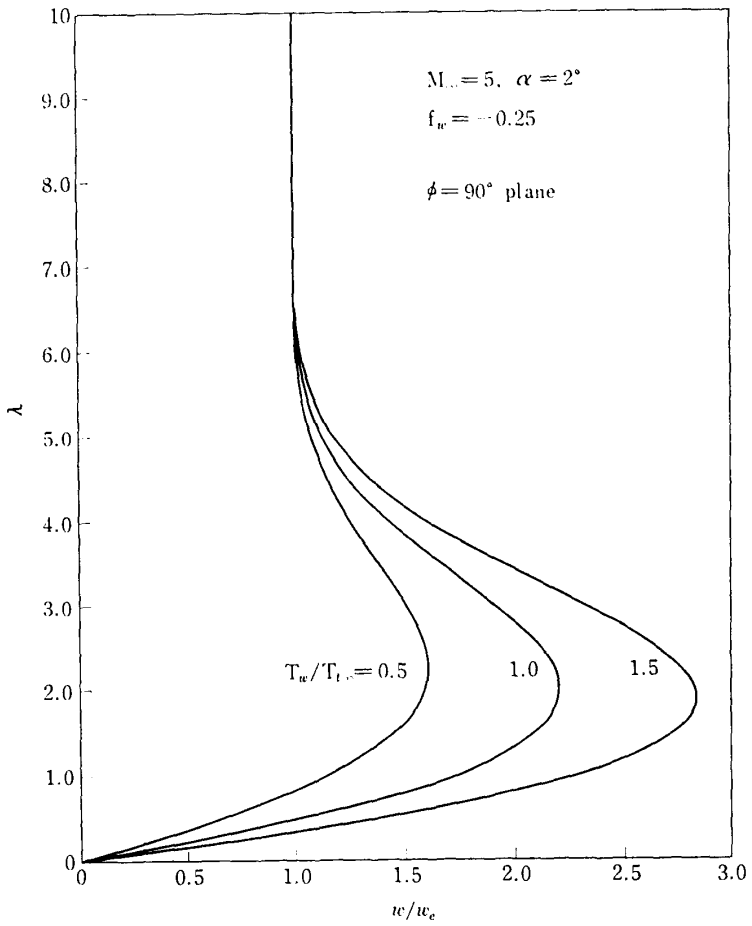

FIG. 9. Profiles of circumferential velocity component for various wall temperatures; 10° circular cone

ature is increased, the circumferential velocity component is greater in magnitude than in the cold wall case. As is pointed out in Ref. [19], this is physically reasonable, since the cooler the wall, the greater the fluid density near the wall and hence, in order to satisfy the requirement of the mass and momentum conservation, the circumferential velocity component is not so great in magnitude as in the hot wall case.

Non-circular cones at angles of attack: As examples of non-circular cones, we deal with following three models:

$$\text{model 2; } \theta = \theta_b(\varphi) = \bar{\theta}_b + \varepsilon_2 \cos 2\varphi \tag{6.1}$$

$$\text{model 3; } \theta = \theta_b(\varphi) = \bar{\theta}_b + \varepsilon_3 \cos 3\varphi \tag{6.2}$$

$$\text{model 4; } \theta = \theta_b(\varphi) = \bar{\theta}_b + \varepsilon_4 \cos 4\varphi \tag{6.3}$$

Eq. (6.1), the model 2, represents an elliptic cone of which the ratio b/a of the major axis and the minor axis is $\tan(\bar{\theta}_b - \varepsilon_2)/\tan(\bar{\theta}_b + \varepsilon_2)$.

The results for the elliptic cone case are presented in Figs. 10–12. Flowfield is shown by means of streamlines in Fig. 10, in which the dashed lines show the limiting

streamlines starting from $\phi=45°$ and $50°$ for the no injection case. The local heat transfer distribution and meridional skin friction distribution are shown in Figs. 11 and 12, respectively. The distribution is non-dimensionalized by $\tilde{q}_0$ (or $\tilde{\tau}_{x0}$), which is the local heat transfer (or meridional skin friction) for the basic circular cone at zero angle of attack in the case of no injection. The peak pressure occurs at $\phi=47.9°$, yet peak heating occurs at $\phi=82°$. As is pointed out [*18*], the peak heating seems to lie between the value of ϕ at the pressure peak (windward side) and the major axis ($\phi=90°$), and the peak meridional skin friction also does. The local heat transfer distributions for the cases of the triangular shaped cone (model 3) and the

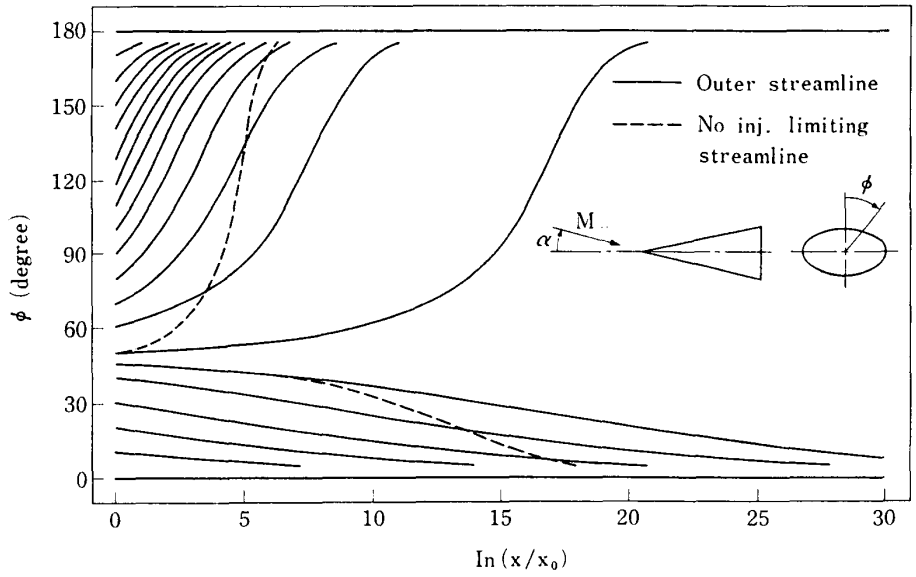

FIG. 10. Streamlines; elliptic cone, $b/a=1.23$, $M_\infty=5$, $\alpha=2°$, $T_w/T_{t\infty}=0.35$ (no injection)

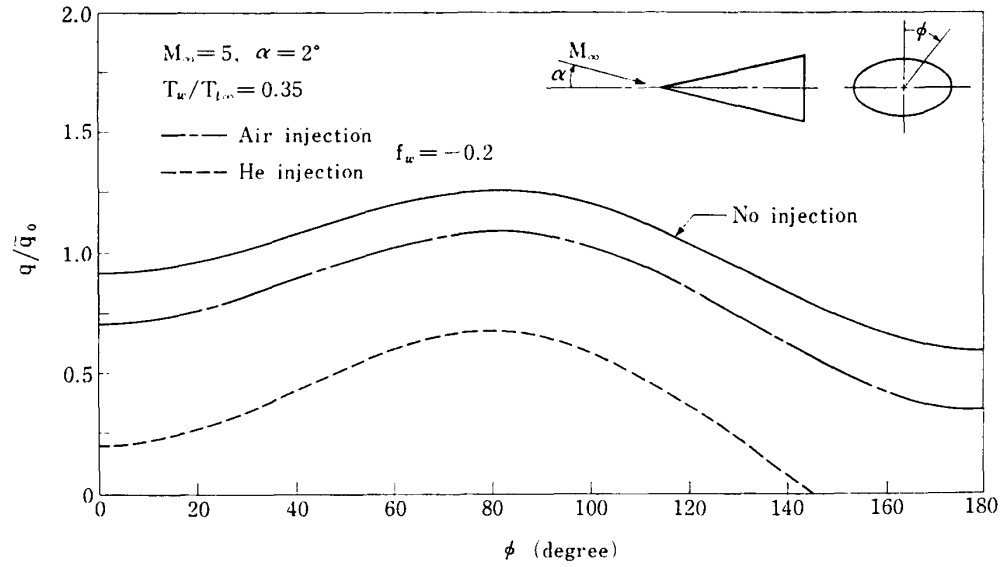

FIG. 11. Effect of mass injection on heat transfer; elliptic cone, $b/a=1.23$

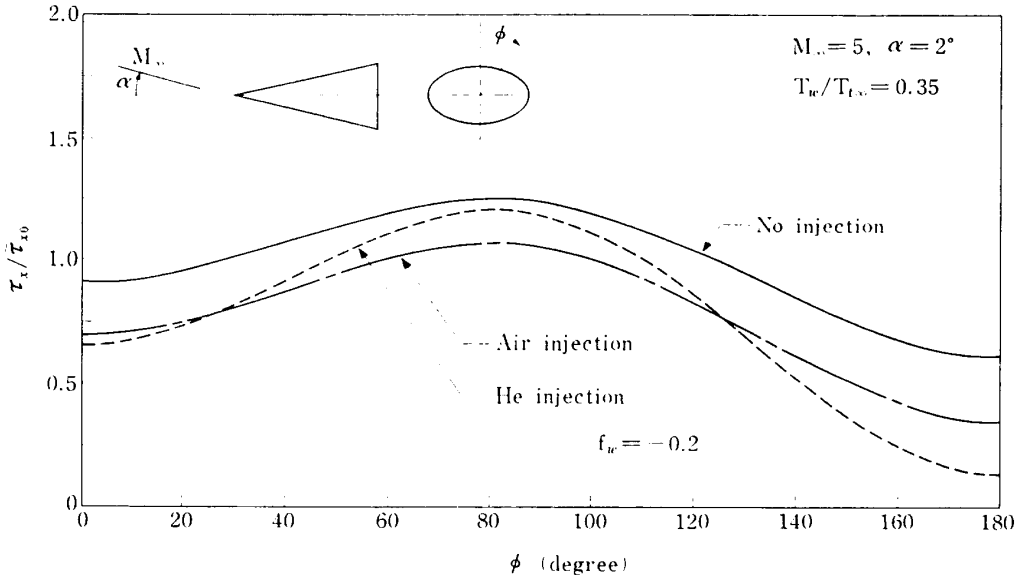

FIG. 12. Effect of mass injection on meridional skin friction; elliptic cone, $b/a=1.23$

rectangular shaped cone (model 4) are shown in Figs. 13 and 14, in which the local heat transfer q is non-dimensionalized by $\tilde{q}_0$, i.e., the local heat transfer of the unyawed basic circular cone without mass injection. With these figures, the peak heating also lies between the value of ϕ at the windward side and the major axis ($\phi=120°$ of model 3, or $\phi=45°$ of model 4). The basic mechanism of the flow over the non-circular cones is likely the same as that infered on the analogy of the yawed circular cone case. However, what seems to be most important for non-circular cone case, the peak heating and the peak skin friction do not occur at windward side.

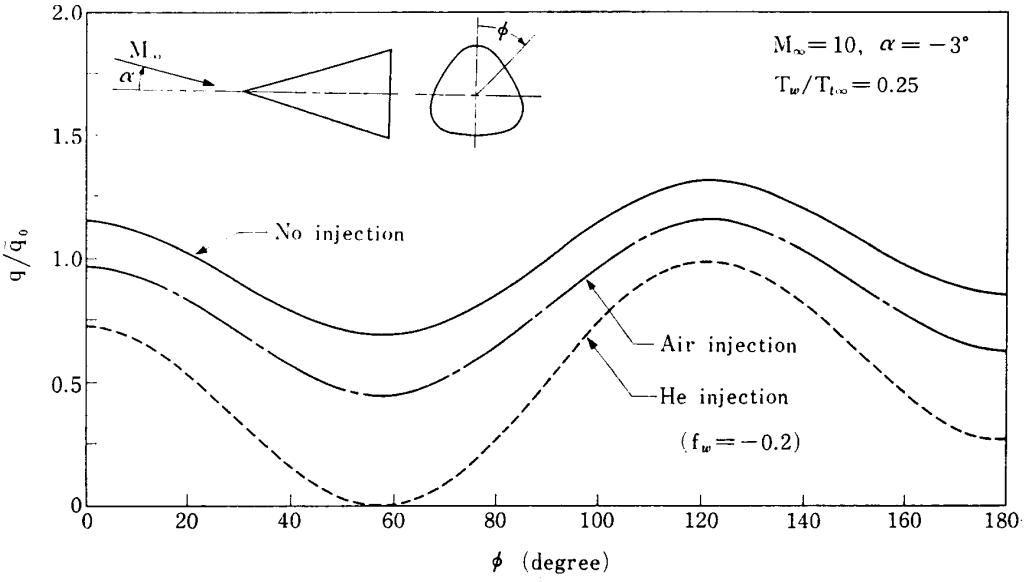

FIG. 13. Effect of mass injection on heat transfer; model 3, $\theta_b=15°+1.0°\cos 3\phi$

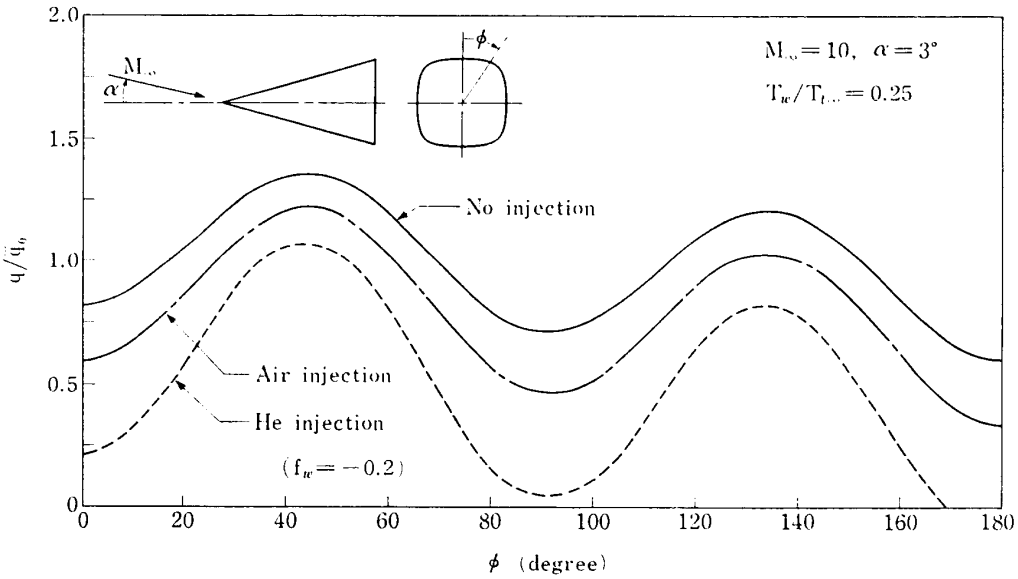

FIG. 14. Effect of mass injection on heat transfar; model 4, $\theta_b = 15° - 0.75° \cos 4\phi$

5. CONCLUSIONS

The three-dimensional, compressible, laminar boundary layer with and without foreign gas injection has been analyzed using small perturbation method. The first order, exact, similar solution is presented in the form not depending on flow parameters. For the circular cone without mass injection at angles of attack, the comparisons of the predicted local heat transfer with the experimental data as well as those calculated by existing numerical methods demonstrate the validity of the present theoretical approach. The influence of mass injection (air-to-air, or helium-to-air) on three-dimensional boundary layer characteristics has been investigated. The following results have been obtained:

(1) The major effect of mass injection is to reduce the local heat transfer and skin friction because of the increase of boundary layer thickness together with change in temperature and velocity profiles across the boundary layer. In the case of the circular cone at small angles of attack, the reduction of local heat transfer is more remarkable on the leeward side than on the windward side.

(2) The maximum value of the cross-flow velocity component increases with increasing mass injection rates. This value in the case of the helium injection is at least two times as great in magnitude as in the case of the air injection. Thus, the helium injection influences more significantly on the three-dimensional character of the boundary layer than the air injection.

(3) In the cases of non-circular cones, such as the elliptic cone, at angles of attack, no points at which the local heat transfer and the meridional skin friction have maximum values coincide with the windward side at which the peak pressure occurs.

The present solution is exact and is, therefore, of interest in itself as well in providing the initial values for a theoretical study of the downstream influence.

Acknowledgement

The authors wish to express their sincere thanks to Prof. H. Oguchi and Prof, K. Karashima for their advices and instructive comments on this study.

Department of Aerodynamics and Structures
Institute of Space and Aeronautical Science
University of Tokyo
Octover 6, 1978

References

[1] Dwyer, H. A.: "Boundary Layer on a Hypersonic Sharp Cone at Small Angle of Attack," AIAA J., Vol. 9, (1971), 277–284.
[2] Moore, F. K.: "Laminar Boundary Layer on a Circular Cone in Supersonic Flow at Small Angle of Attack," NACA TN-2521, (1951).
[3] Moore, F. K.: "Laminar Boundary Layer on Cone in Supersonic Flow at Large Angle of Attack," NACA Rept. 1132, (1953).
[4] Wuest, W.: "Kompressible Laminare Zweistoffgrenzschichten," Z. Flugwiss, Vol. 11, (1963), 398–409, (in German).
[5] Libby, P. A.: "Three-Dimensional Boundary Layer with Uniform Mass Transfer," The Physics of Fluid, Vol. 12, (1969), 408–417.
[6] Marvin, J. G. and Sheaffer, Y. S.: "A Method for Solving the Nonsimilar Laminar Boundary Layer Equations Including Foreign Gas Injection," NASA TND-5516, (1969).
[7] Wortman, A.: "Heat and Mass Transfer on Cones at Angles of Attack," AIAA J., Vol. 10, (1972), 832–834.
[8] Wortman, A.: "Foreign Gas Injection at Windwardmost Meridians of Yawed Sharp Cones," AIAA J., Vol. 12, (1974), 741–742.
[9] Matsuno, K. and Kawamura, R.: "Laminar Boundary Layer with Gas Injection on a Conical Body," Bulletin of ISAS, Univ. of Tokyo, Vol. 13, (1977), 685–717, (in Japanese).
[10] Jaffe, N. A., Lind, R. C. and Smith, A. M. O.: "Solution to the Binary Diffusion Laminar Boundary Layer Equations with Second-Order Transverse Curvature," AIAA J., Vol. 5, (1967), 1563–1569.
[11] Stone, A. H.: "On Supersonic Flow past a Slightly Yawing Cone," J. Math. and Phys., Vol. 27, (1948), 67–81.
[12] Ferri, A.: "Supersonic Flow around Circular Cones at Angles of Attack," NACA TN-2236, (1950).
[13] Stocker, P. M. and Mauger, F. F.: "Supersonic Flow past Cones of General Cross-section," J. Fluid Mech., Vol. 13, (1962), 383–399.
[14] Ferri, A., Ness, N. and Kaplita, T. T.: "Supersonic Flow over Conical Bodies without Axial Symmetry," J. Aero. Sci., Vol. 20, (1953), 563–571.
[15] Taylor, G. I. and Maccoll, J. W.: "The Air Pressure on a Cone Moving at High Speeds," Proc. Roy. Soc. (A), Vol. 139, (1933), 278–311.
[16] Holt, M. and Blackie, J.: "Experiments on Circular Cones at Yaw in Supersonic Flow," J. Aero. Sci., Vol. 23, (1956), 931–936.
[17] Tracy, R. R.: "Hypersonic Flow over a Yawed Circular Cone," GALCIT Memo., No. 69, (1963).
[18] McGowan, J. J. III and Davis, R. T.: "Development of a Numerical Method to Solve the Three-Dimensional Compressible Laminar Boundary Layer Equations with Application to Elliptical Cones at Angle of Attack," ARL 70-0341, (1970).
[19] Kang, S.-W., Rae, W. J. and Dunn, M. G.: "Effects of Mass Injection on Compressible, Three-Dimensional, Laminar Boundary Layers," AIAA J., Vol. 5, (1967), 1738–1745.